SIMULATIONS OF LIMITING CURRENT IN A CROSSED-FIELD GAP: HULL DIODE

by

J. P. Verboncoeur and C. K. Birdsall

Memorandum No. UCB/ERL M93/86

15 December 1993

SIMULATIONS OF LIMITING CURRENT IN A CROSSED-FIELD GAP: HULL DIODE

by

J. P. Verboncoeur and C. K. Birdsall

Memorandum No. UCB/ERL M93/86

15 December 1993

ELECTRONICS RESEARCH LABORATORY

College of Engineering
University of California, Berkeley
94720

SIMULATIONS OF LIMITING CURRENT IN A CROSSED-FIELD GAP: HULL DIODE

by

J. P. Verboncoeur and C. K. Birdsall

Memorandum No. UCB/ERL M93/86

15 December 1993

ELECTRONICS RESEARCH LABORATORY

College of Engineering
University of California, Berkeley
94720

Simulations of Limiting Current in a Crossed-Field Gap: Hull Diode

J. P. Verboncoeur and C. K. Birdsall
ERL and EECS Dept., University of California, Berkeley, CA 94720
December 15, 1993

ABSTRACT. Simulations confirm the Hull cutoff [1] as the limiting stable current for a space charge limited planar crossed-field diode. In addition, a current occurs beyond the Hull cutoff, with a near-zero average value plus a high frequency oscillatory component which dies rapidly in time. The diode reacts strongly to small increases in injection current above the current limit and magnetic field above the Hull cutoff, with a rapid reduction of transmitted current. The simulations are performed in 1D3V, using PDP1 [2].

This work was performed with support from the Air Force Office of Scientific Research under grant F49620-92-J0487.

Introduction

Recently, Lau, Christenson and Chernin [3] have re-interpreted the Hull cutoff as the limiting current for a planar crossed-field diode. The cutoff is well known; a summary is in the text by Birdsall and Bridges [4], drawing upon the work of Pollack [5]; see also the references in [3] and [6]. For space charge limited current, Pollack showed infinite slopes in transit angle, transit time and velocity as the Hull limit is approached. These results are shown in Figure 1. Note that in Figure 1d, the slope of the current at Hull cutoff does not appear to be infinite, although this can be shown from the expressions in Pollack [5]. The infinite slope was shown to be the case analytically by Lau et. al. [3]. The infinite slopes lead one to suspect instability as the Hull limit is crossed; this interpretation was shown to be the case for the unmagnetized diode in [4].

It is not clear to Birdsall why he and Bridges did not identify limiting current for the magnetized diode (after studying the limiting current in the unmagnetized diode in 1959) when including the work of Pollack in their text [4].

The concept of limiting electron current in diodes and drift tubes has its roots in the 1930's, with values calculated from time-independent analyses (see, for example, [7] and [8]). The study of average and oscillatory currents beyond limiting current awaited modern computational tools; an early example is in [4], Chapter 3.

Hence, when the Hull cutoff was proposed as the crossed-field limiting current, we were stimulated to study both the cutoff and beyond, using existing kinetic particle simulation tools. In particular, we look for virtual cathode oscillations beyond the cutoff, as found earlier in the unmagnetized diode by Birdsall and Bridges [4].

Case 1: Unmagnetized Child-Langmuir Diode

Initially, we revisited the planar unmagnetized Child-Langmuir diode, since the limiting current in the Hull diode can be related to Child-Langmuir current in an unmagnetized diode [3,5]. This model provides a stable current up to the Child-Langmuir limit. Electrons are emitted from the cathode (left electrode of Figure 2) into a vacuum diode. The anode is grounded, and the cathode is held at -10 kV with respect to the anode, with no impedance in the external circuit. The diode gap is 1 cm, and the electrode area is 1 cm^2. For these dimensions and potential, J_{CL} = 2.33 A/cm^2. The simulation requires an initial velocity for the electrons injected (to avoid $\rho \rightarrow \infty$ at the cathode), so we inject a cold beam at 0.5 eV. The simulation confirms that the entire injected current is transmitted; the anode current is J_{CL}. The fluctuations in diode space charge density, field, and potential are negligible. The usual Child law variations in position x are observed: potential $\Phi \sim x^{4/3}$, electric field $E \sim x^{1/3}$, and density $\rho \sim x^{-2/3}$.

Case 2: Critical Current Injection at Hull Field

Next, we applied a static magnetic field perpendicular to the diode gap, ψ = 90 degrees in Figure 2. The injection current was reduced to the limiting current at the Hull field, $9/4\pi\ J_{CL}$ = 1.6687 A/cm^2 as shown in Figure 1d. The remaining parameters of Case 1 are retained. The value chosen is the Hull cutoff field [1],

$$B_H = \frac{m}{eD}\sqrt{\frac{2eV}{m} + u_0^2}\ ,$$

where V is the applied voltage, D is the diode gap separation, and u_0 is the initial velocity of the beam. For u_0 small or zero, this is equivalent to setting the electron gyroradius at the anode velocity equal to the diode gap, D. For our configuration, B_H = 337 Gauss.

The result is a stable, non-oscillatory system. The anode current is equal to the injected current, as shown in Figure 3. From the phase space plot, we see the electrons never quite reach the turning point, $v_x = 0$, at the anode. The potential for this case is proportional to $x^{1.47}$, in comparison with the $x^{4/3}$ of the unmagnetized diode.

Although stability is the analytically predicted result, it is remarkable that neither the turn-on transient nor the statistical noise of the particle-in-cell simulation drives the instability. We will show below that a very small increase in cathode current or magnetic field is sufficient to alter the behavior of the diode radically. Since we inject a finite number of PIC particles, N, we might expect a variation in current about the mean value which scales as $N^{-1/2}$. For this case, N is on the order of 3000 PIC particles, and we see no noise problems.

Case 3: Critical Current Injection at 1% Above Hull Field

Starting from Case 2, we increased the magnetic field by 1% above the Hull field, to 340 Gauss. As shown in Figure 4, initially the current increases to $9/4\pi\ J_{CL}$ just as in Case 2. However, once that current value is reached, the diode undergoes a rapid transition to a current oscillating about zero. The transition occurs in under 3.9 ns. The oscillations, at 330 MHz, damp in time to zero.

For comparison, the plasma frequency is 1.0 GHz, the cyclotron frequency is 950 MHz and the hybrid frequency is 1.4 GHz. It is unclear why the current oscillates at the low frequency. The plot of the number of electrons in the diode gap shows a similar oscillation at 330 MHz, with a high frequency modulation at 3.4 GHz. In addition, the potential at the center of the gap oscillates about its mean value at 330 MHz modulated at the cyclotron frequency. The spatial potential here is proportional to $x^{1.93}$.

We do not observe the small average currents beyond the cutoff reported by Hull [1], although those curves are for the cylindrical case. Further investigation at $B/B_H = 1.1$ provides a similar result, with a transition to the decaying current oscillations occuring in less than 1 ns.

Case 4: Injection 1% Above Critical Current at Hull Field

Starting again from Case 2, we increased the injection current by 1% above the critical value, to $J = 1.685$ A/cm^2. The results are shown in Figure 5. The current ramps up to the critical value as in Case 2, and remains stable for about 45 ns. During this time, the space charge density in the gap is gradually increasing. The transmitted current then makes a rapid transition to a new mean value of about 10% of the critical current. The transition takes about 14 ns. In both regimes, the current exhibits either noise or oscillatory behavior of a few percent of the mean value. The number of electrons in the gap after the transition oscillates at 1.2 GHz, and the potential at the center of the gap oscillates at 1.0 GHz. The potential varies spatially in proportion to $x^{1.78}$. The plasma frequency and cyclotron frequency are both 940 Mhz, and the hybrid frequency is 1.3 GHz.

Case 5: Child-Langmuir Injection at Hull Field

For this case, we increase the injection current to $J = J_{CL}$, with all other parameters identical to Case 4. The results are shown in Figure 6. The anode current behaves similarly to that of Case 4, with an inital ramp up to the critical current, followed by a 12 ns transition to a final state of about 10% of the critical current. The current in all regimes also exhibits oscillatory or noisy behavior of a few percent of the mean value. The potential varied in proportion to $x^{1.78}$, just as in Case 4. The electron density in the gap was slightly lower than Case 4 (7.1×10^9 cm^{-3} versus 1.1×10^{10} cm^{-3}), leading to an electron plasma frequency of 760 MHz. The hybrid frequency is 1.2 GHz. In this case, the number of electrons in the gap oscillates at 2.8 GHz, and the potential at the center of the gap oscillates at the hybrid frequency.

The balance of the injected charge returns to the cathode, with return velocities much larger than the injected values. The electron energy increase, sufficient to generate secondary emission from the cathode, is only possible with a time-varying potential. Note that we have neglected secondary emission in these simulations.

Conclusions

We have characterized the planar crossed-field diode near the the Hull cutoff using particle-in-cell simulation. The diode is stable for injection at the critical current. The simulations verify the predicted current limit. A transition to a reduced current occurs for a small increase of injection

current above the critical current at the Hull cutoff. In addition, we observed a transition to a current oscillating about zero and decaying in time for an applied magnetic field above the Hull cutoff. The high frequency oscillations described here have previously been characterized as noise [5].

The rapid transition in anode current initiated by a small increase in either injection current or applied transverse magnetic field indicates potential use as a rapid current switching device. The transition time and related behavior can be controlled by scaling the voltage, applied magnetic field, and dimensions of the diode. Such a device may be useful for rapid switching in high current or voltage conditions, such as in power switching or surge protection.

Further Study

Further study of the crossed-field diode near the Hull cutoff is warranted. Specifically, the curve of limiting current versus magnetic field can be characterized using simulation. One can choose values of $B/B_H < 1$ and gradually ramp up J to find the onset of current transition. By mapping out the regions of space charge limited current, the entire limiting current curve can be verified. Similarly, B/B_H can be increased from 0 with $J/J_{CL} = 1$. Possible hysteresis can be observed by decreasing J and B after the onset of instability.

The value of the external circuit parameters can be varied to investigate device characteristics above limiting current and beyond the Hull cutoff. For example, one may find microwave oscillation near $\omega^2_{resonant} = 1/LC$, with some additional considerations for the RC and L/R time constants of the circuit. Early work on instability in the unmagnetized diode showed a maximum efficiency of less than 1%, so no device work was pursued [4]. However, virtual cathode oscillators (vircators) currently produce up to terrawatts of pulsed power, albeit at low efficiency. Therefore, one may find a useful device in spite of low efficiency.

The parallel and perpendicular cathode emission temperatures may affect limiting current and the dynamics of the instability. In addition, the diode behavior may change for gap potentials much smaller than 10 kV, where cathode temperature is not negligible compared to the gap voltage.

The dynamics of a cylindrical Hull diode can be studied using PDC1 [2]. This code provides cylindrical inner and outer electrodes, so comparison to cylindrical diode noise studies in the literature is possible.

The observed energy of the electron flux returning to the cathode was large, on the order of the gap voltage. This can be a serious issue for cathode lifetime, particularly in the presence of a background gas. Secondary electron emission may also play a role in the diode kinetics; investigation of both the energy and angular distribution of the returning electrons is warranted.

In addition, more careful study of the current limited regimes may yield information on the sources of noise in crossed-field devices.

REFERENCES

1. A. W. Hull, "Effect of a uniform magnetic field on the motion of electrons between coaxial cylinders," *Phys. Rev.* **18**, 31-57 (1921).

2. PDP1 (Plasma Device Planar 1 Dimensional) and PDC1 (Plasma Device Cylindrical 1 Dimensional), © 1990-93 Regents of the University of California, Plasma Theory and Simulation Group, Berkeley, CA. Available from Software Distribution Office of the ILP, 205 Cory Hall, Berkeley, CA 94720, software@eecs.Berkeley.EDU.

3. Y. Y. Lau, P. J. Christenson and D. Chernin, "Limiting Current in a Crossed-Field Gap," *Phys. Fluids* **5**, 4486 (1993).

4. C. K. Birdsall and W. B. Bridges, *Electron Dynamics of Diode Regions*, Academic Press (1966).

5. M. A. Pollack, *Noise Transport in the Crossed-Field Diode*, Ph.D. Thesis, University of California, Berkeley, CA, Series No. 60, Issue No. 485 (1962).

6. J. W. Gewartowski and H. A. Watson, *Principles of Electron Tubes*, D. Van Nostrand (1965). See esp. pp. 431-436.

7. C. E. Fay, A. L. Samuel and W. Shockly, "On the theory of space charge between parallel plane electrodes," *Bell Syst. Tech. J.* **17**, 49-47 (1938).

8. B. Salzberg and A. V. Haeff, "Effects of space charge in the grid-anode region of vacuum tubes," *R.C.A. Rev.* **2**, 336-374 (1938).

Figure Captions

Figure 1. Magnetized space charge limited planar diode (a) transit angle, (b) transit time, (c) anode velocity, and (c) current as a function of magnetic field. Here, $B_c = B_H$, and u_a is a small initial velocity at the cathode. From Pollack [5] via [4].

Figure 2. Simulation model for PDP1 [2]. For the crossed-field diode, $\psi = 90°$. Displacements are in x only, velocities are v_x and v_y. Here we use D = 1 cm, electrode area of 1 cm^2, V = -10 kV, and $R = L = 0$, C = 1 F (a DC-biased short circuit).

Figure 3. Case 2: $B/B_H = 1$, injected current $J/J_{CL} = 9/4\pi$. This case is predicted to be stable. Potential (not shown) varied spatially as $x^{1.47}$ in comparison to $x^{4/3}$ of the unmagnetized diode.

Figure 4. Case 3: $B/B_H = 1.01$, injected current $J/J_{CL} = 9/4\pi$. Experiments in this region indicate noisy operation; our results show noise and decaying oscillations. Potential (not shown) varied spatially as $x^{1.93}$ in comparison to $x^{4/3}$ of the unmagnetized diode.

Figure 5. Case 4: $B/B_H = 1$, injected current $J/J_{CL} = 1.01\text{x}9/4\pi$. Potential (not shown) varied spatially as $x^{1.78}$ in comparison to $x^{4/3}$ of the unmagnetized diode.

Figure 6. Case 5: $B/B_H = 1$, injected current $J/J_{CL} = 1$. Potential (not shown) varied spatially as $x^{1.78}$ in comparison to $x^{4/3}$ of the unmagnetized diode.

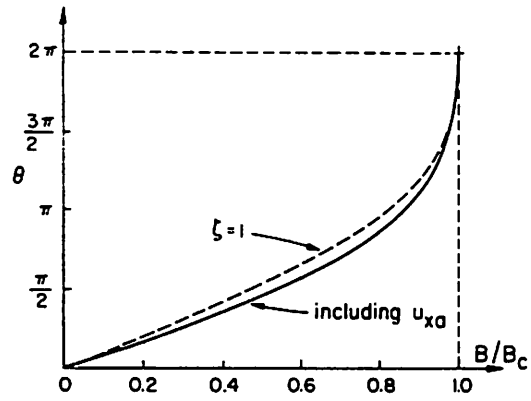

a. Transit angle θ as a function of magnetic field B [from Pollack (1962)].

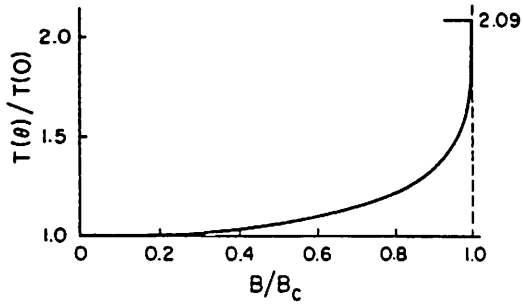

b. Transit time as a function of magnetic field B [from Pollack (1962)].

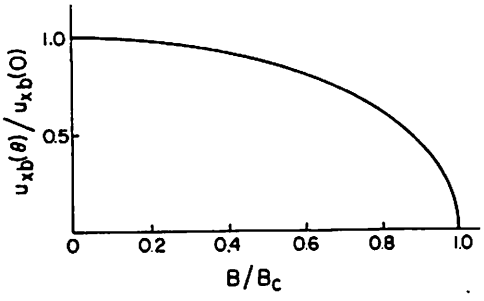

c. Velocity as a function of magnetic field B [from Pollack (1962)].

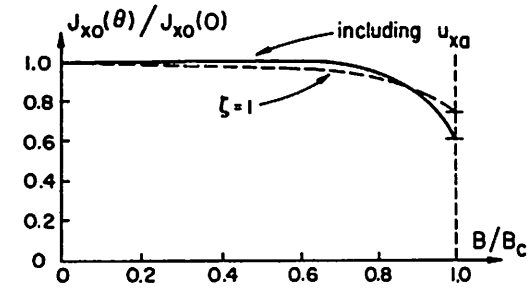

d. Current as a function of magnetic field B [from Pollack (1962)].

Figure 1.

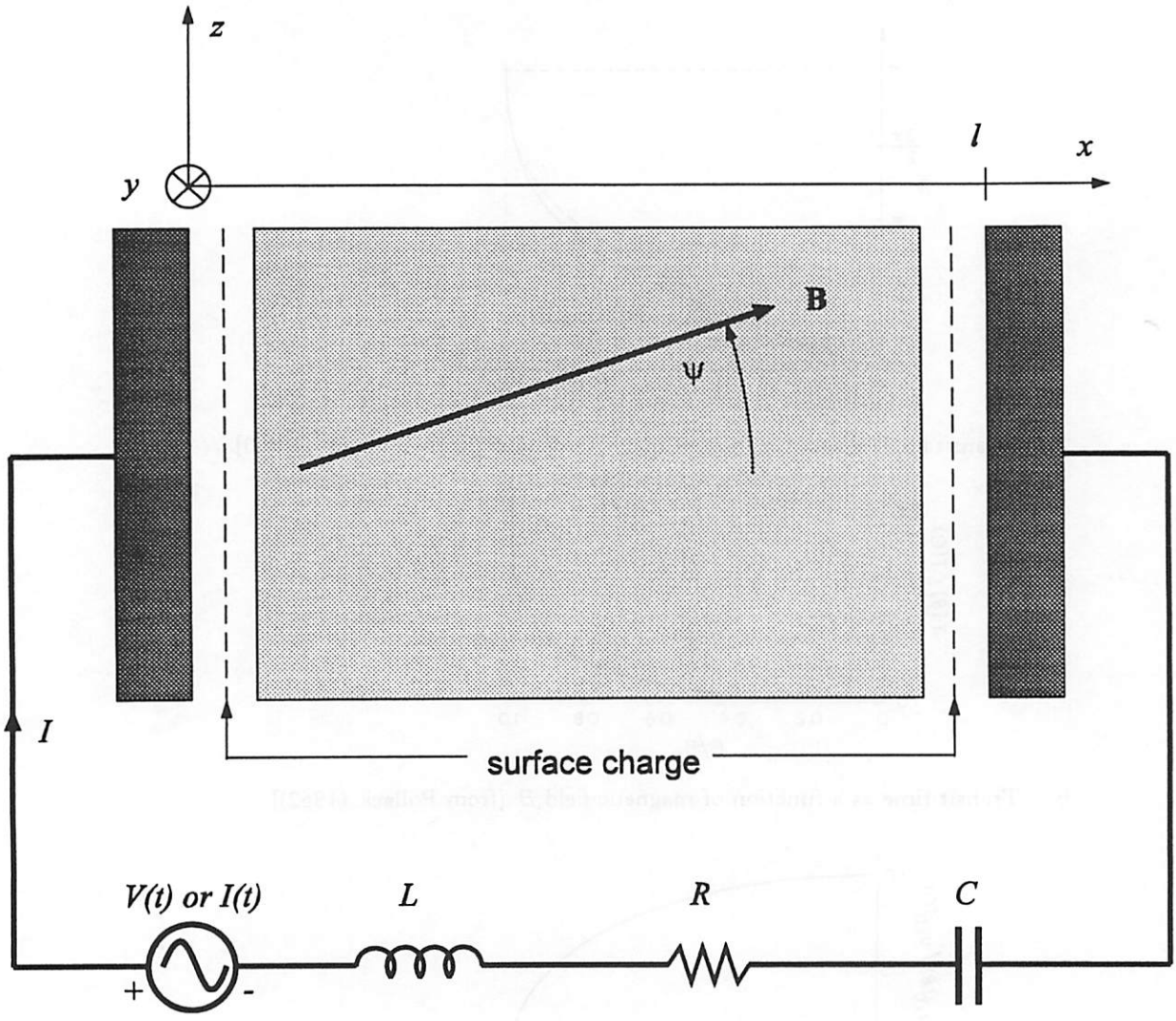

Figure 2.

Figure 3.
Case 2.

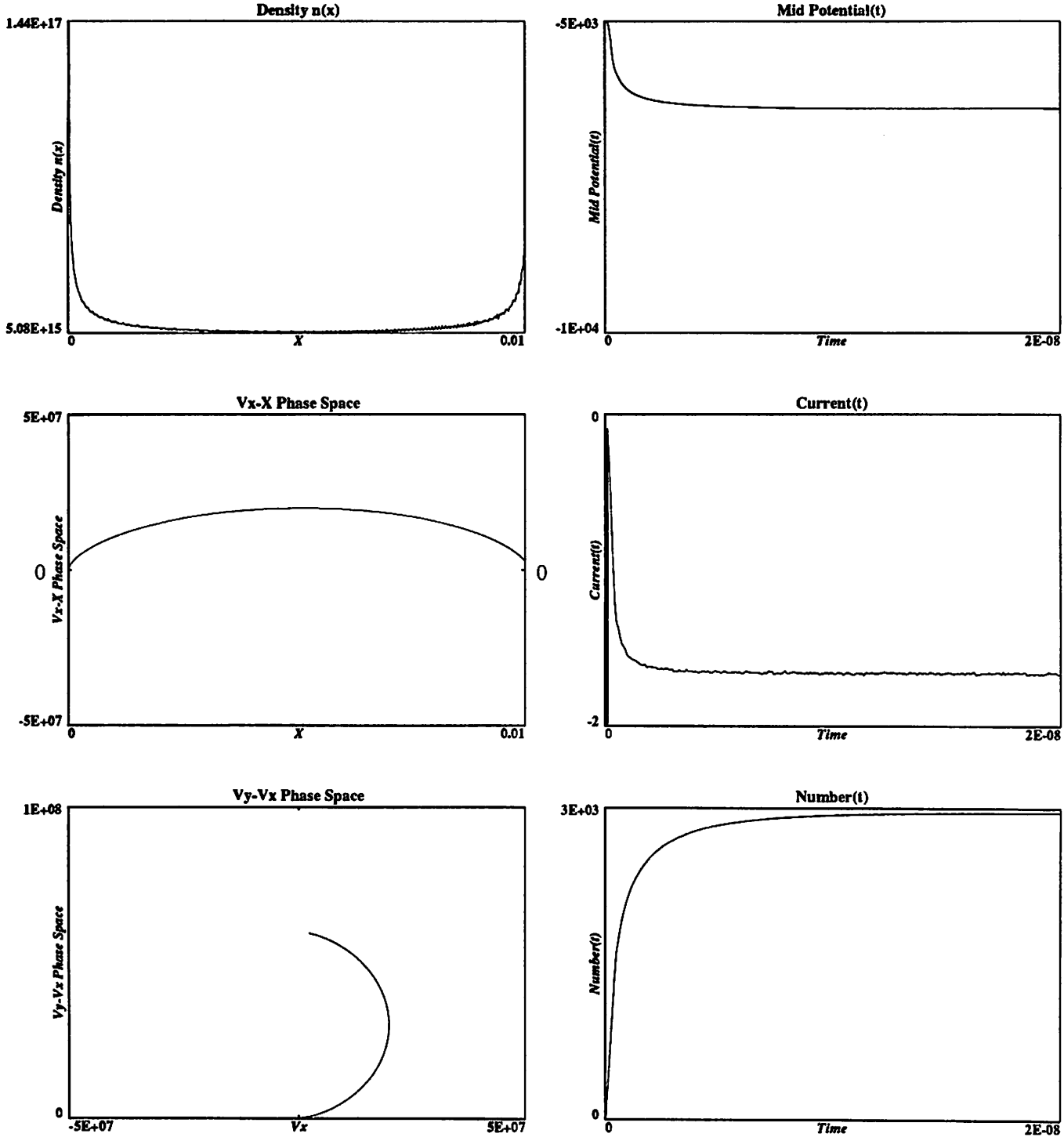

Figure 4.
Case 3.

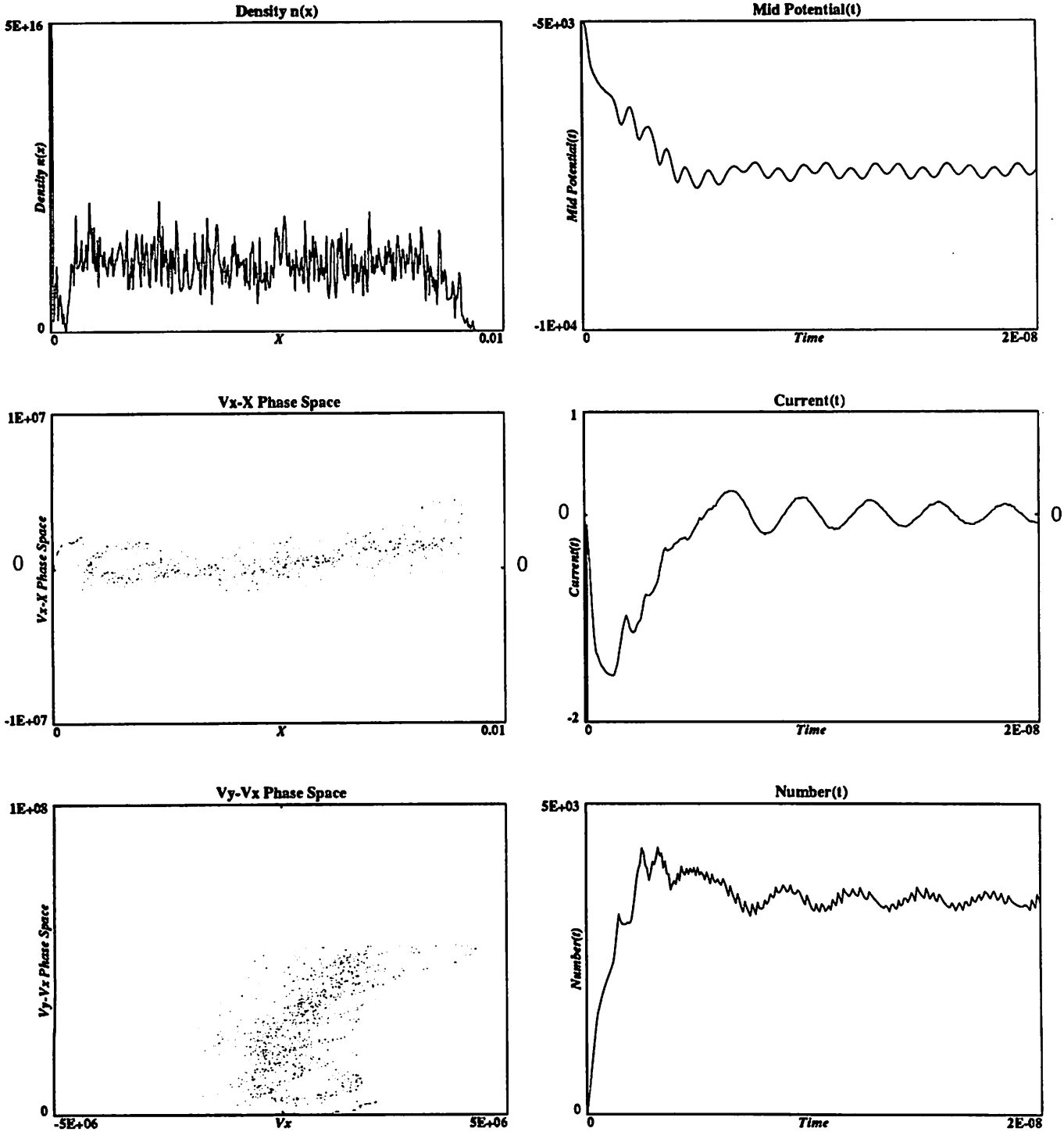

Figure 5.
Case 4.

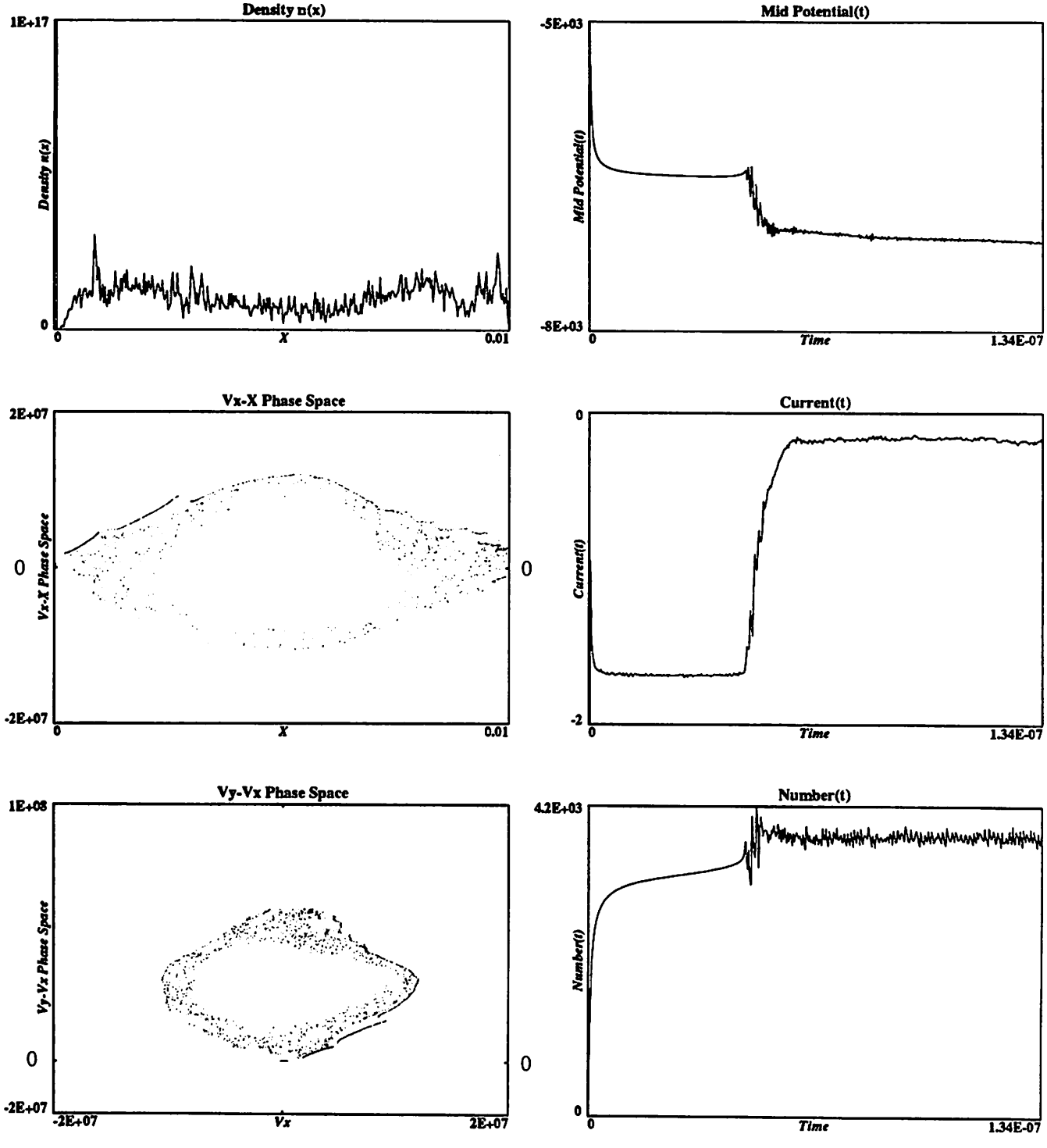

Figure 6.
Case 5.